SCIENCE CHINA
Technological Sciences

• Article •

June 2016 Vol.59 No.6: 941–952
doi: 10.1007/s11431-016-6054-x

# A generalized $L_2$-discrepancy for cubature and uncertainty quantification of nonlinear structures

CHEN JianBing[1*] & SONG PengYan[2]

[1] *State Key Laboratory of Disaster Reduction in Civil Engineering & School of Civil Engineering, Tongji University, Shanghai 200092, China*
[2] *College of Civil Engineering and Architecture, Hebei University, Baoding 071002, China*

Received March 18, 2015; accepted November 28, 2015; published online May 3, 2016

The numerical method for multi-dimensional integrals is of great importance, particularly in the uncertainty quantification of engineering structures. The key is to generate representative points as few as possible but of acceptable accuracy. A generalized $L_2(GL_2)$-discrepancy is studied by taking unequal weights for the point set. The extended Koksma-Hlawka inequality is discussed. Thereby, a worst-case error estimate is provided by such defined $GL_2$-discrepancy, whose closed-form expression is available. The characteristic values of $GL_2$-discrepancy are investigated. An optimal strategy for the selection of the representative point sets with a prescribed cardinal number is proposed by minimizing the $GL_2$-discrepancy. The three typical examples of the multi-dimensional integrals are investigated. The stochastic dynamic response analysis of a nonlinear structure is then studied by incorporating the proposed method into the probability density evolution method. It is shown that the proposed method is advantageous in achieving tradeoffs between the efficiency and accuracy of the exemplified problems. Problems to be further studied are discussed.

**Koksma-Hlawka inequality, cubature, $L_2$-discrepancy, nonlinear structure, stochastic dynamics**

**Citation:** Chen J B, Song P Y. A generalized $L_2$-discrepancy for cubature and uncertainty quantification of nonlinear structures. Sci China Tech Sci, 2016, 59: 941–952, doi: 10.1007/s11431-016-6054-x

## 1 Introduction

High-dimensional integrals are frequently encountered in science and engineering disciplines [1–3]. In many cases, the closed-form solutions of such high-dimensional integrals are not readily available because the integrand may be in a very complex form or even could only be obtained by numerical methods. For instance, in uncertainty quantification or stochastic dynamics of engineering structures, the dynamic response, as a function of the basic random parameters, usually could only be evaluated by solving the high-dimensional nonlinear equations of equilibrium or motion resulting from the finite element discretization, which further involves the solution of the complex constitutive laws in structural or geotechnical engineering [4–7]. Therefore, numerical methods for such problems, usually referred to as quadrature when the dimension is not greater than 2 and as cubature when the dimension is greater than 3, are of great concern and extensively studied for decades, resulting in a variety of approaches.

Roughly speaking, these approaches could be classified into two classes: The ones based on some kind of best reachable accuracy defined by the highest degree, to which the cubature formula of polynomials could yield exact value, and the ones based on some kind of worst-case error estimate, which is governed by the family of Koksma-Hlawka inequalities. The approaches belonging to the first class include, for example, different forms of Gaussian formulae and the sparse grids in high dimensions [2]. Such approach-

*Corresponding author (email:chenjb@tongji.edu.cn)

es have been successfully applied in uncertainty quantification for some problems [8,9]. However, many kinds of sparse grids, such as the Smolyak scheme [10] and the complete symmetric grids [11], possess negative weights. This might be satisfactory in many problems, but may not be preferred in uncertainty quantification where the concept of probability implies positive weights, and some spurious numerical results may occur due to negative weights [12]. In these cases, the schemes with positive weights are preferred and studied by some researchers [13,14].

The approaches belonging to the second class could usually be sub-divided into those generating point sets "randomly" and those generating point sets in a deterministic manner. The former is well known as the Monte Carlo method and the latter is usually referred to as the number-theoretical method [15,16] or quasi-Monte Carlo (QMC) method [17,18]. The methods in the former sub-class may suffer from the low convergence rate and random convergence in nature, which are improved or circumvented in the methods belonging to the latter sub-class. In this context, the concept of discrepancy plays an essential role, which in a sense guarantees a worst-case error in a deterministic sense [1]. Thus, to find low-discrepancy point sets is one of the central tasks. Along this line, fruitful results have been achieved in the past decades, a lot of low-discrepancy point sets (such as Sobol' points, digital (*t*-*α*-*m*-*s*) nets) were found and widely applied [15,19].

Most researches are focused on equal-weight cubature formulae and the corresponding discrepancy [18]. From the point of view of the practical applications in some fields, the uncertainty quantification of structural responses in civil, mechanical and offshore or marine engineering [20], the concept of unequal probabilities is natural due to the almost surely non-uniform/non-homogenous discretization. Actually, as mentioned by researchers [18,21–23], the unequal weights are feasible, but few investigations are available for applications. In addition, in engineering practical applications, the deterministic analysis is usually computationally expensive, at least taking 10 h or more for one single deterministic analysis of a practical structure with about one million degrees of freedom. It is therefore urgently desired that the cardinal number of the point sets, i.e., the number of the deterministic function evaluations, should be limited to the order of a magnitude of 300, or preferably less. This raises the problem of tackling cubature or large-scale uncertainty quantification issues with a small number of deterministic evaluations. The unequal-weight schemes may provide more feasibility and flexibility.

In the present paper, the cubature formulae with unequal weights will be studied and illustrated in stochastic dynamics of multi-degree-of-freedom (MDOF) nonlinear structures. The paper will be organized as follows. In Section 2, the concept of $L_2$-discrepancy and its counterpart with unequal weights, the generalized $L_2$-discrepancy ($GL_2$-discrepancy for short) will first be introduced. Next, the extended Koksma-Hlawka inequality will be discussed in the case involving non-equal weights with the corresponding $GL_2$-discrepancy by invoking the reproducing kernel Hilbert space theory. The closed-form expressions of $GL_2$-discrepancy in one and multiple dimensions will be given. In Section 3, the characteristic values of $GL_2$-discrepancy are discussed. In Section 4, the optimization problem of selecting the coordinates of representative point sets together with the corresponding unequal weights are described. The algorithm will be illustrated in the integral of typical functions to demonstrate its properties in Section 5. Last, in this section the proposed method will be applied in the stochastic dynamic analysis of an MDOF nonlinear structure by incorporating into the probability density evolution method. Problems to be further studied are discussed.

## 2 $L_2$- and generalized $L_2$-discrepancy

### 2.1 Partitioning of unit hypercube and unequal weights

In many science and engineering disciplines, it is of great concern to evaluate the following high-dimensional integral

$$I(f)=\int_{C^s} f(\boldsymbol{x})\mathrm{d}\boldsymbol{x}, \tag{1}$$

where $C^s=[0,1]^s$ is the *s*-dimensional unit hypercube, and $f(\boldsymbol{x})=f(x_1,\cdots,x_s)$ is an *s*-dimensional function. If the function $f$ is of variation bounded, then the celebrated Koksma-Hlawka inequality exists when the integral is approximated by a sample mean, i.e., [15,17]

$$\left|I(f)-S_n(f)\right|\leqslant D^*(M_n)\cdot V(f), \tag{2}$$

where

$$S_n(f)=\frac{1}{n}\sum_{k=1}^{n} f(\boldsymbol{x}_k) \tag{3}$$

is the widely adopted quadrature (cubature) formula, *n* is the cardinal number of the point set $M_n=\{\boldsymbol{x}_k\in C^s\}_{k=1}^n$, $D^*(M_n)$ is the star discrepancy which is only dependent on the point set $M_n$, and $V(f)$ is the total variation of the function *f* in the sense of Hardy and Krause, which essentially characterizes the degree of irregularity of the hyper-surface $f(\boldsymbol{x})$. Note that in eq. (3) equal weights of 1/*n* are adopted for each function value.

The integral in eq. (1) could be treated in an alternative way by partitioning the unit hypercube into subdomains $\Omega_1,\Omega_2,\cdots,\Omega_n$, which satisfy $\bigcup_{k=1}^n\Omega_n=C^s$ and $\mathrm{vol}\{\Omega_k\bigcap\Omega_m\}=0$ for $\forall k\neq m$, where $\mathrm{vol}\{\cdot\}$ denotes the Lebesgue measure (area or volume) of the domain. Therefore, it follows from eq. (1) that

$$I(f)=\int_{C^s} f(\boldsymbol{x})\mathrm{d}\boldsymbol{x}=\sum_{k=1}^{n}\int_{\Omega_k} f(\boldsymbol{x})\mathrm{d}\boldsymbol{x}. \tag{4}$$

According to the mean value theorem, for continuous function there must be some points in each sub-domain $\tilde{\boldsymbol{x}}_k\in\Omega_k, k=1,2,\cdots,n$ that make $\sum_{k=1}^{n}\int_{\Omega_k} f(\boldsymbol{x})\mathrm{d}\boldsymbol{x}=\sum_{k=1}^{n} f(\tilde{\boldsymbol{x}}_k)\int_{\Omega_k}1\mathrm{d}\boldsymbol{x}=\sum_{k=1}^{n}a_k f(\tilde{\boldsymbol{x}}_k)$ hold exactly. Here $a_k=\int_{\Omega_k}1\mathrm{d}\boldsymbol{x}$ is the Lebesgue measure of $\Omega_k$. In this sense, these points could be referred to as representative points, and the sub-domains referred to as representative domains. In practice, because such 'exact' representative points are difficult to be located and will be different for different integrands, for some chosen points $\boldsymbol{x}_k\in\Omega_k, k=1,2,\cdots,n$, there is an approximation

$$I(f)\approx Q_n(f)=\sum_{k=1}^{n} f(\boldsymbol{x}_k)\left(\int_{\Omega_k}1\mathrm{d}\boldsymbol{x}\right)=\sum_{k=1}^{n}a_k f(\boldsymbol{x}_k), \tag{5}$$

where as before $a_k=\int_{\Omega_k}1\mathrm{d}\boldsymbol{x}=\mathrm{vol}\{\Omega_k\}$. Clearly, $0<a_k<1$ for all *k*, and $\sum_{k=1}^{n}a_k=1$.

As mentioned, $M_n=\{\boldsymbol{x}_k\in C^s\}_{k=1}^{n}$ is the representative point set, and $\Omega_k$'s are the corresponding representative domains. Particularly, in uncertainty quantification or stochastic dynamics, the integral in eq. (1) is actually the mean of a random function $f(\boldsymbol{X})=f(X_1,\cdots,X_s)$ when $\boldsymbol{X}=(X_1,\cdots,X_s)$ is a random vector with independent identically distributed components uniformly distributed over [0,1]. In this case, $a_k=\mathrm{vol}\{\Omega_k\}$ could be understood as the probability $a_k=\Pr\{\boldsymbol{X}\in\Omega_k\}$, where $\Pr\{\cdot\}$ is the probability of the bracketed event. Thereby, $a_k$'s could also be called the assigned probabilities [20,24]. Evidently, if $a_k$'s are forced to be 1/*n*, $Q_n(f)$ defined in eq. (5) reduces to $S_n(f)$ defined in eq. (3).

The major task of the present paper is to prove the counterpart of inequality (2) when the unequal weights (assigned probabilities) are adopted and give the explicit expression for the discrepancy.

For an extended F-discrepancy defined by

$$D_{\mathrm{EF}}(M_n)=\sup_{\boldsymbol{x}\in C^s}\left|\sum_{k=1}^{n}a_k u(\boldsymbol{x}_k-\boldsymbol{x})-\mathrm{vol}[0,\boldsymbol{x}]\right|, \tag{6}$$

where $\boldsymbol{x}=(x_1,\cdots,x_s)$, $\mathrm{vol}[0,\boldsymbol{x}]=\prod_{j=1}^{s}x_j$, and $u(\boldsymbol{x}_k-\boldsymbol{x})=\prod_{j=1}^{s}u(x_{k,j}-x_j)$, in which $u(z)$ is Heaviside's function with the value being 1 if $z\geqslant 0$ and zero otherwise, it is proven that Inequality (2) still holds when $S_n(f)$ and $D^*(M_n)$ are replaced by $Q_n(f)$ and $D_{\mathrm{EF}}(M_n)$, respectively [14,25]. This is an extension of the classical version of Koksma-Hlawka inequality for unequal weights. In the present paper, the $L_2$-discrepancy will be extended to involve the effects of unequal weights, and the Koksma-Hlawka inequality for the $GL_2$-discrepancy will be justified.

## 2.2 Extension of the Koksma-Hlawka inequality for $L_2$-discrepancy in multiple dimensions

### *2.2.1 Closed-form expression for $GL_2$-discrepancy in multiple dimensions*

According to the reproducing kernel space theory [19], if there are some functions $K(x,y)$ satisfying

$$f(y)=\langle f,K(\cdot,y)\rangle, \tag{7}$$

where $\langle\cdot\rangle$ denotes the inner product of two functions, then $K(x,y)$ is a reproducing kernel. If we let

$$K(x,y)=1+\min(1-x,1-y), \tag{8}$$

and define the inner product of two functions *f* and *g* as

$$\langle f,g\rangle=f(1)g(1)+\int_0^1 f'(x)g'(x)\mathrm{d}x, \tag{9}$$

where $f'(x)=\partial f/\partial x$ and $g'(x)=\partial g/\partial x$, it could be verified that eq. (7) holds and thus $K(x,y)$ defined in eq. (8) could serve as a reproducing kernel [19].

Assume the integral of an *s*-dimensional function $f(\boldsymbol{x})=f(x_1,\cdots,x_s)$ and the cubature formula are defined as in eqs. (1) and (5), respectively, i.e.,

$$I(f)=\int_{C^s} f(\boldsymbol{x})\mathrm{d}\boldsymbol{x},\quad Q_n(f)=\sum_{k=1}^{n}a_k f(\boldsymbol{x}_k), \tag{10}$$

where $M_n=\{\boldsymbol{x}_k=(x_{k,1},\cdots,x_{k,d},\cdots,x_{k,s})\in C^s\}_{k=1}^{n}$ is the representative point set and $a_k$'s are the unequal weights (assigned probabilities).

Define a multi-dimensional reproducing kernel function $K(\boldsymbol{x},\boldsymbol{y})$ satisfying

$$f(\boldsymbol{y})=\langle f,K(\cdot,\boldsymbol{y})\rangle, \tag{11}$$

where $\boldsymbol{x}=(x_1,\cdots,x_s)$, $\boldsymbol{y}=(y_1,\cdots,y_s)$.

A tensor product of the one-dimensional kernels could be adopted to construct the multi-dimensional reproducing kernel [19]

$$K(\boldsymbol{x},\boldsymbol{y})=\prod_{d=1}^{s}K(x_d,y_d)=\prod_{d=1}^{s}[1+\min(1-x_d,1-y_d)], \tag{12}$$

and the inner product is defined analogous to, but is an extension of eq. (9) in multiple dimensions.

Using eq. (11), we have

$$\begin{aligned} I(f)-Q_N(f) &= \int_{C^s} f(\boldsymbol{x})\mathrm{d}\boldsymbol{x}-\sum_{k=1}^{n} a_k f(\boldsymbol{x}_k) \\ &= \int_{C^s} \langle f, K(\cdot,\boldsymbol{y})\rangle \mathrm{d}\boldsymbol{y}-\sum_{k=1}^{n} a_k \langle f, K(\cdot,\boldsymbol{x}_k)\rangle \\ &= \left\langle f, \int_{C^s} K(\cdot,\boldsymbol{y})\mathrm{d}\boldsymbol{y}\right\rangle - \left\langle f, \sum_{k=1}^{n} a_k K(\cdot,\boldsymbol{x}_k)\right\rangle \\ &= \left\langle f, \int_{C^s} K(\cdot,\boldsymbol{y})\mathrm{d}\boldsymbol{y}-\sum_{k=1}^{n} a_k K(\cdot,\boldsymbol{x}_k)\right\rangle. \end{aligned} \tag{13}$$

Let

$$h(\boldsymbol{x};M_n)=\int_{C^s} K(\cdot,\boldsymbol{y})\mathrm{d}\boldsymbol{y}-\sum_{k=1}^{n} a_k K(\cdot,\boldsymbol{x}_k). \tag{14}$$

From eq. (13) it follows by invoking the Cauchy-Schwarz inequality that

$$\left|I(f)-Q_N(f)\right| = \left|\langle f,h\rangle\right| \leqslant \|h\|_2 \|f\|_2. \tag{15}$$

Define the $\mathrm{GL}_2$-discrepancy in multiple dimensions by

$$L_2^{\mathrm{uw}}(M_n)=\|h(\boldsymbol{x};M_n)\|_2=\sqrt{\langle h,h\rangle}. \tag{16}$$

We have the following theorem.

**Theorem 1**. If $f(\boldsymbol{x})$ is a bounded function with finite first mixture derivatives in $C^s$ and a cubature formula $Q_n(f)=\sum_{k=1}^{n} p_k f(\boldsymbol{x}_k)$ is adopted to approximate the integral $I(f)=\int_{C^s} f(\boldsymbol{x})\mathrm{d}\boldsymbol{x}$, then the error is bounded by the following inequality

$$\left|I(f)-Q_n(f)\right| \leqslant L_2^{\mathrm{uw}}(M_n)\cdot\|f\|_2, \tag{17}$$

where the $\mathrm{GL}_2$-discrepancy $L_2^{\mathrm{uw}}(M_n)$ is defined by eq. (16), and $\|f\|_2$ is the 2-norm of the integrand.

*2.2.2 Closed-form expression for $\mathrm{GL}_2$-discrepancy in multiple dimensions*

The closed-form expression of the $\mathrm{GL}_2$-discrepancy in multiple dimensions could also be obtained without essential difficulty. To this end, substituting eq. (14) in eq. (16) yields

$$\begin{aligned} &\left(L_2^{\mathrm{uw}}(M_n)\right)^2 \\ &= \|h\|_2^2 \\ &= \left\langle \int_{C^s} K(\boldsymbol{x},\boldsymbol{y})\mathrm{d}\boldsymbol{y}-\sum_{k=1}^{n} a_k K(\boldsymbol{x},\boldsymbol{x}_k), \right. \\ &\quad \left. \int_{C^s} K(\boldsymbol{x},\boldsymbol{y})\mathrm{d}\boldsymbol{y}-\sum_{k=1}^{n} a_k K(\boldsymbol{x},\boldsymbol{x}_k)\right\rangle \\ &= \left\langle \int_{C^s} K(\boldsymbol{x},\boldsymbol{y})\mathrm{d}\boldsymbol{y}, \int_{C^s} K(\boldsymbol{x},\boldsymbol{y})\mathrm{d}\boldsymbol{y}\right\rangle \\ &\quad -2\left\langle \int_{C^s} K(\boldsymbol{x},\boldsymbol{y})\mathrm{d}\boldsymbol{y}, \sum_{k=1}^{n} a_k K(\boldsymbol{x},\boldsymbol{x}_k)\right\rangle \\ &\quad +\left\langle \sum_{k=1}^{n} a_k K(\boldsymbol{x},\boldsymbol{x}_k), \sum_{k=1}^{n} a_k K(\boldsymbol{x},\boldsymbol{x}_k)\right\rangle \\ &= \int_{C^s}\int_{C^s} \langle K(\cdot,\boldsymbol{x}), K(\cdot,\boldsymbol{y})\rangle \mathrm{d}\boldsymbol{x}\mathrm{d}\boldsymbol{y} \\ &\quad -2\sum_{k=1}^{n} a_k \int_{C^s} \langle K(\cdot,\boldsymbol{y}), K(\cdot,\boldsymbol{x}_k)\rangle \mathrm{d}\boldsymbol{y} \\ &\quad +\sum_{i=1}^{n}\sum_{j=1}^{n} a_i a_j \langle K(\cdot,\boldsymbol{x}_i), K(\cdot,\boldsymbol{x}_j)\rangle \\ &= \int_{C^s}\int_{C^s} K(\boldsymbol{x},\boldsymbol{y})\mathrm{d}\boldsymbol{x}\mathrm{d}\boldsymbol{y} \\ &\quad -2\sum_{k=1}^{n} a_k \int_{C^s} K(\boldsymbol{x}_k,\boldsymbol{y})\mathrm{d}\boldsymbol{y}+\sum_{i=1}^{n}\sum_{j=1}^{n} a_i a_j K(\boldsymbol{x}_i,\boldsymbol{x}_j). \end{aligned} \tag{18}$$

For the reproducing kernel in eq. (12), we have $\int_{C^s}\int_{C^s} K(\boldsymbol{x},\boldsymbol{y})\mathrm{d}\boldsymbol{x}\mathrm{d}\boldsymbol{y}=\left(\frac{4}{3}\right)^s$ and $\int_{C^s} K(\boldsymbol{x}_k,\boldsymbol{y})\mathrm{d}\boldsymbol{y}=\prod_{d=1}^{s}\left(1+\frac{1-x_{k,d}^2}{2}\right)$. Substituting these results in eq. (18) immediately leads to

$$\begin{aligned} L_2^{\mathrm{uw}}(M_n) = \Bigg\{ &\left(\frac{4}{3}\right)^s -2\sum_{k=1}^{n} a_k \prod_{d=1}^{s}\left(1+\frac{1-x_{k,d}^2}{2}\right) \\ &+\sum_{i=1}^{n}\sum_{j=1}^{n} a_i a_j \prod_{d=1}^{s}[1+\min(1-x_{i,d},1-x_{j,d})]\Bigg\}^{1/2}. \end{aligned} \tag{19}$$

This result could also be found as a special case in ref. [22]. Clearly, if the weights are forced to take equal values $1/n$, then eq. (19) reduces to

$$\begin{aligned} L_2^{\mathrm{uw}}(M_n) = \Bigg\{ &\left(\frac{4}{3}\right)^s -\frac{2}{n}\sum_{k=1}^{n} \prod_{d=1}^{s}\left(1+\frac{1-x_{k,d}^2}{2}\right) \\ &+\frac{1}{n^2}\sum_{i=1}^{n}\sum_{j=1}^{n} \prod_{d=1}^{s}[1+\min(1-x_{i,d},1-x_{j,d})]\Bigg\}^{1/2}. \end{aligned} \tag{20}$$

This is exactly the $\mathrm{L}_2$-discrepancy in multiple dimensions given in ref. [19].

## 3 Characteristic values of $\mathrm{GL}_2$-discrepancy

For convenience, denote the square of $\mathrm{GL}_2$-discrepancy by

$$\begin{aligned} D_2 &= [L_2^{\mathrm{uw}}(M_n)]^2 \\ &= \left(\frac{4}{3}\right)^s -2\sum_{k=1}^{n} a_k \prod_{d=1}^{s}\left(1+\frac{1-x_{k,d}^2}{2}\right) \end{aligned}$$

$$+\sum_{i=1}^{n}\sum_{j=1}^{n}a_i a_j\prod_{d=1}^{s}[1+\min(1-x_{i,d},1-x_{j,d})]. \tag{21}$$

In the case all the points are 'randomly' scattered and all the unequal weights are also 'randomly' valued, then $D_2$ is also a random variable. To be clear, all the coordinates $x_{i,d}$ for $i=1,\cdots,n,\ d=1,\cdots,s$ are independent random variables uniformly distributed over $[0,1]^s$, whereas $p_1,\cdots,p_n$ are random variables uniformly distributed over the hyper-plane $\Omega_a=\{(a_1,\cdots,a_n)\,|\,\sum_{i=1}^{n}a_i=1,\ \text{and}\ 0\leqslant a_i\leqslant 1\}$ with the joint probability density function (PDF)

$$p_{a_1\cdots a_n}(a_1,\cdots,a_n)=\begin{cases}\dfrac{1}{\mathrm{vol}(\Omega_a)},\ \text{for}\ (a_1,\cdots,a_n)\in\Omega_a,\\ 0,\ \text{otherwise},\end{cases} \tag{22}$$

where $\mathrm{vol}(\Omega_a)=\dfrac{\sqrt{n}}{(n-1)!}$ is the Lebesgue measure of the domain $\Omega_a$.

It is not at all a trivial task to obtain the PDF of $D_2$. Instead, the mean value of $D_2$ could be evaluated as follows:

$$\begin{aligned}E[D_2]&=E\left\{\left(\frac{4}{3}\right)^s-2\sum_{k=1}^{n}a_k\prod_{d=1}^{s}\left(1+\frac{1-x_{k,d}^2}{2}\right)\right.\\&\quad\left.+\sum_{i=1}^{n}\sum_{j=1}^{n}a_i a_j\prod_{d=1}^{s}[1+\min(1-x_{i,d},1-x_{j,d})]\right\}\\&=\left(\frac{4}{3}\right)^s-2\sum_{k=1}^{n}E[a_k]\prod_{d=1}^{s}E\left(1+\frac{1-x_{k,d}^2}{2}\right)\\&\quad+\sum_{i=1}^{n}E[a_i^2]\prod_{d=1}^{s}E(2-x_{i,d})\\&\quad+\sum_{i=1}^{n}\sum_{j=1,j\neq i}^{n}E[a_i a_j]\prod_{d=1}^{s}E[\min(2-x_{i,d},2-x_{j,d})].\end{aligned} \tag{23}$$

Note that $E[x_{k,d}]=\dfrac{1}{2}$, $E[x_{k,d}^2]=\dfrac{1}{3}$, and

$$\begin{aligned}E[\min(2-x_{i,d},2-x_{j,d})]&=2-E[\max(x_{i,d},x_{j,d})]\\&=2-\int_0^1\int_0^1\max(x,y)\mathrm{d}x\mathrm{d}y\\&=\frac{4}{3}.\end{aligned} \tag{24}$$

Eq. (23) becomes

$$\begin{aligned}E[D_2]&=\left(\frac{4}{3}\right)^s-2\sum_{k=1}^{n}E[a_k]\left(\frac{4}{3}\right)^s+\left(\frac{3}{2}\right)^s\sum_{i=1}^{n}E[a_i^2]\\&\quad+\left(\frac{4}{3}\right)^s\sum_{i=1}^{n}\sum_{j=1,j\neq i}^{n}E[a_i a_j]\\&=\left[\left(\frac{3}{2}\right)^s-\left(\frac{4}{3}\right)^s\right]E\left\{\sum_{k=1}^{n}a_k^2\right\}.\end{aligned} \tag{25}$$

Because $\sum_{k=1}^{n}a_k^2\leqslant\sum_{k=1}^{n}a_k=1$, we have the first bound as follows:

$$0<E[D_2]\leqslant\left(\frac{3}{2}\right)^s-\left(\frac{4}{3}\right)^s. \tag{26}$$

In the case $s=1$, there is $0<E[D_2]\leqslant 1/6$.

### 3.1 Random point coordinates and deterministic weights

Let us consider the situation when the weights are deterministic but undetermined. In this case, eq. (25) becomes

$$E[D_2]=\left[\left(\frac{3}{2}\right)^s-\left(\frac{4}{3}\right)^s\right]\gamma(a_1,\cdots,a_n), \tag{27}$$

where $\gamma(a_1,\cdots,a_n)=\sum_{k=1}^{n}a_k^2$. According to the optimization principle, to find the minimum $\gamma(a_1,\cdots,a_n)=\sum_{k=1}^{n}a_k^2$ under the constraint $\sum_{k=1}^{n}a_k=1$, and $0\leqslant a_k\leqslant 1$ is a problem of quadratic programming with constraints [26]. This problem is well-posed and the minimum value exists and is unique when $a_1=a_2=\cdots=a_n=1/n$. In this case, $\min_{(a_1,\cdots,a_n)\in\Omega_a}\gamma(a_1,\cdots,a_n)=1/n$, and therefore

$$\min_{(a_1,\cdots,a_n)\in\Omega_a}E[D_2]=\frac{1}{n}\left[\left(\frac{3}{2}\right)^s-\left(\frac{4}{3}\right)^s\right]. \tag{28}$$

This means that in the case the coordinates of points are randomly scattered, the equal weights will yield a minimum mean value of $D_2$. In addition, it is seen that $\min_{(a_1,\cdots,a_n)\in\Omega_a}E[D_2]$ decreases in the order of magnitude of $\mathcal{O}(n^{-1})$ as $n$ increases, this means that the $\min_{(a_1,\cdots,a_n)\in\Omega_a}E[L_2^{\mathrm{uw}}]=\min_{(a_1,\cdots,a_n)\in\Omega_a}E[\sqrt{D_2}]$ will decrease in the order of the magnitude of $\mathcal{O}(n^{-1/2})$ as $n$ increases, as will be verified by the numerical examples later.

### 3.2 Random point coordinates and random weights

Now come back to eq. (25), i.e.,

$$E[D_2]=\left[\left(\frac{3}{2}\right)^s-\left(\frac{4}{3}\right)^s\right]E[\gamma(a_1,\cdots,a_n)], \tag{29}$$

where

$$E[\gamma(a_1,\cdots,a_n)]=\int_{\Omega_a}\left(\sum_{k=1}^{n}a_k^2\right)p_{a_1\cdots a_n}(a_1,\cdots,a_n)\mathrm{d}a_1\cdots\mathrm{d}a_n$$
$$=n\int_{\Omega_a}a_1^2\,p_{a_1\cdots a_n}(a_1,\cdots,a_n)\mathrm{d}a_1\cdots\mathrm{d}a_n$$
$$=nE[a_1^2]=\cdots=nE[a_n^2]. \tag{30}$$

It is noted that $a_1,\cdots,a_n$ are not independent random variables, and thus although due to the symmetry there is $E[a_1^2]=\cdots=E[a_n^2]$, it is no easy job to find the exact values of $E[a_k^2]$. It could be argued that $E[a_k]=n^{-1}$, and correspondingly $E[a_k^2]\sim\mathcal{O}(n^{-2})$, and there should exist $E[\gamma(a_1,\cdots,a_n)]\sim\mathcal{O}(n^{-1})$. This is verified by the numerical results in Figure 1.

Here it is noted that $E[\gamma(a_1,\cdots,a_n)]$ is greater than $\min\limits_{(a_1,\cdots,a_n)\in\Omega_a}\gamma(a_1,\cdots,a_n)=1/n$, , which is actually expected, because if we let $a_k=\dfrac{1}{n}-\beta_k$ then we have

$$E[\gamma(a_1,\cdots,a_n)]=E\left[\sum_{k=1}^{n}a_k^2\right]=E\left[\sum_{k=1}^{n}\left(\frac{1}{n}-\beta_k\right)^2\right]$$
$$=\frac{1}{n}+E\left[\sum_{k=1}^{n}\beta_k^2\right]>\frac{1}{n},$$

where use has been made of $E\left[\sum\limits_{k=1}^{n}\beta_k\right]=0$. Clearly, $E[\beta_k^2]=E\left[\left(a_k-\dfrac{1}{n}\right)^2\right]=E[(a_k-E(a_k))^2]$ is nothing but the variance of $a_k$. This is clearly understandable because $\min\limits_{(a_1,\cdots,a_n)\in\Omega_a}\gamma(a_1,\cdots,a_n)=1/n$ is the minimum value of $\gamma(a_1,\cdots,a_n)$ for all possible $(a_1,\cdots,a_n)\in\Omega_a$, no matter deterministic or random. The mean value $E[\gamma(a_1,\cdots,a_n)]$ of course shall be greater than the minimum value.

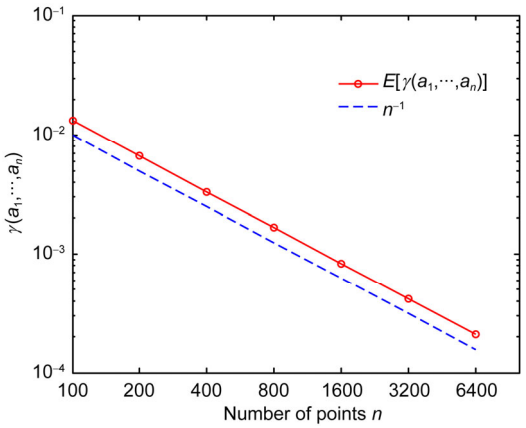


**Figure 1** (Color online) The tendency of $\gamma$ v.s. $n$.

However, it should be stressed that only the mean of $D_2$ is discussed, whereby the tendency could be observed. This in no sense implies that for "randomly" scattered points and "randomly" assigned weights $D_2$ will reach its minimum when all the weights are equal. Actually, the unequal weights will take advantage over the equal weights for practical use.

## 4 Optimal determination of point sets by minimizing $GL_2$-discrepancy

In many science and engineering disciplines, the deterministic function evaluation as involved in the cubature formula eq. (10) is much time consuming. For instance, as mentioned in the introduction, in structural dynamics of civil, mechanical, aerospace and ocean engineering, huge degrees of freedom in the order of the magnitude of thousands and even millions are usually involved. Besides, nonlinearity will be exhibited in the mechanical behaviors of structures when they are subjected to disastrous excitations such as earthquake, strong wind and huge waves [27]. In such scenarios, it may take at least tens of or more hours to perform one single deterministic analysis. Therefore, for practical applications it is urgent to reduce the number of deterministic function evaluations to the order of 300 or less, but the accuracy should be as high as possible.

To this end, the foregoing theorems provide a theoretical basis. As a matter of fact, Theorem 1 implies that the worst-case errors of the quadrature and cubature formulas are bounded by the $GL_2$-discrepancy. Therefore, if the cardinal number of the representative point set is prescribed as, say $n$ = 200, then the $GL_2$-discrepancy could be taken as an objective function to be minimized, and the coordinates of the point sets and the unequal weights are those to be determined. In other words, for a specified $n$, we are led to the following optimization problem:

$$\min_{x_{k,d},\,p_k\ (k=1,2,\cdots,n;\ d=1,2,\cdots,s)} L_2^{\mathrm{uw}}(M_n)$$
$$=\left\{\left(\frac{4}{3}\right)^s-2\sum_{k=1}^{n}p_k\prod_{d=1}^{s}\left(1+\frac{1-x_{k,d}^2}{2}\right)\right.$$
$$\left.+\sum_{i=1}^{n}\sum_{j=1}^{n}p_ip_j\prod_{d=1}^{s}[1+\min(1-x_{i,d},1-x_{j,d})]\right\}^{1/2} \tag{31}$$
$$\textit{subject to}\quad 0\leqslant x_{k,d}\leqslant 1,$$
$$0<p_k<1,$$
$$\text{and}\quad\sum_{k=1}^{n}p_k=1.$$

In this problem, the number of optimization variables to be determined is $n(s+1)$. If we consider a problem involving

10 random variables and prescribe the number of points $n$=200, then there are 2200 variables to be determined. Of course this is a large-scale problem. Some methods have been developed for such optimization problems [25]. Heuristic optimization approaches, such as the Genetic Algorithm, could also be applied. Alternatively, a two-step optimization adopting the quadrature optimization could be employed [28].

Fortunately, the closed-form objective function in eq. (31) is well defined and could be computed very quickly. Thus, as a straightforward approach, the random searching approach could be implemented very easily. Using this method, the pseudo-random numbers are generated for the variables $x_{k,d}, p_k$ $(k=1,2,\cdots,n;\ d=1,2,\cdots,s)$ and the $\mathrm{GL}_2$-discrepancy $L_2^{\mathrm{uw}}(M_n)$ is then evaluated. After thousands or more rounds of such evaluations are performed, the data with minimal $L_2^{\mathrm{uw}}(M_n)$ will be recorded and adopted as the desired data. Of course, generally this could only lead to sub-optimal rather than optimal results, but it is indeed very simple and effective.

## 5 Numerical examples

### 5.1 Simple cubature

In this sub-section, the integrals of the following three functions

$$\begin{cases} I(f_1)=\int_{C^3} f_1(\boldsymbol{x})\mathrm{d}\boldsymbol{x} \\ =\int_0^1\int_0^1\int_0^1 (2\pi)^{-3/2}\exp\left\{-\dfrac{x_1^2+x_2^3+x_3^2}{2}\right\}\mathrm{d}x_1\mathrm{d}x_2\mathrm{d}x_3, \\ I(f_2)=\int_{C^3} f_2(\boldsymbol{x})\mathrm{d}\boldsymbol{x} \\ =\int_0^1\int_0^1\int_0^1 \ln(1+x_1+x_2+x_3)\mathrm{d}x_1\mathrm{d}x_2\mathrm{d}x_3, \\ I(f_3)=\int_{C^s} f_3(\boldsymbol{x})\mathrm{d}\boldsymbol{x} \\ =\int_0^1\cdots\int_0^1\prod_{d=1}^{s}\dfrac{|4x_d-2|+a_d}{1+a_d}\mathrm{d}x_1\mathrm{d}x_2\cdots\mathrm{d}x_s, \end{cases} \tag{32}$$

are taken to study the performance of the proposed approach. The closed-form solutions of the integrals yield the following values [16,29]

$$\begin{cases} I(f_1)=[\Phi(1)-\Phi(0)]\approx 0.03977, \\ I(f_2)\approx 0.8951, \\ I(f_3)=1. \end{cases} \tag{33}$$

In the present paper, $a_d=1$ for $d=1,2,\cdots,s$ are taken in $f_3$. To be clear, the relative error of a cubature is defined as $e(f;M_n)=\dfrac{|I(f)-Q_n(f)|}{|I(f)|}$.

In Figure 2, pictures are the pairs $(L_2^{\mathrm{uw}}(M_n), e(f,M_n))$ for different point sets with different cardinal numbers (i.e., the number of deterministic function evaluations). 100000 rounds of different point sets are generated randomly for each cardinal number of 200, 400, 800 and 1600, and 10000 rounds of different point sets are generated randomly for the cardinal number of 3200. Therefore there are 100000 data pairs for $n$ = 200 and 10000 data pairs for $n$ = 3200 in the figures. The most remarkable property that is observed in Figure 2(a)–(c) is that all the points are under a line, i.e., an

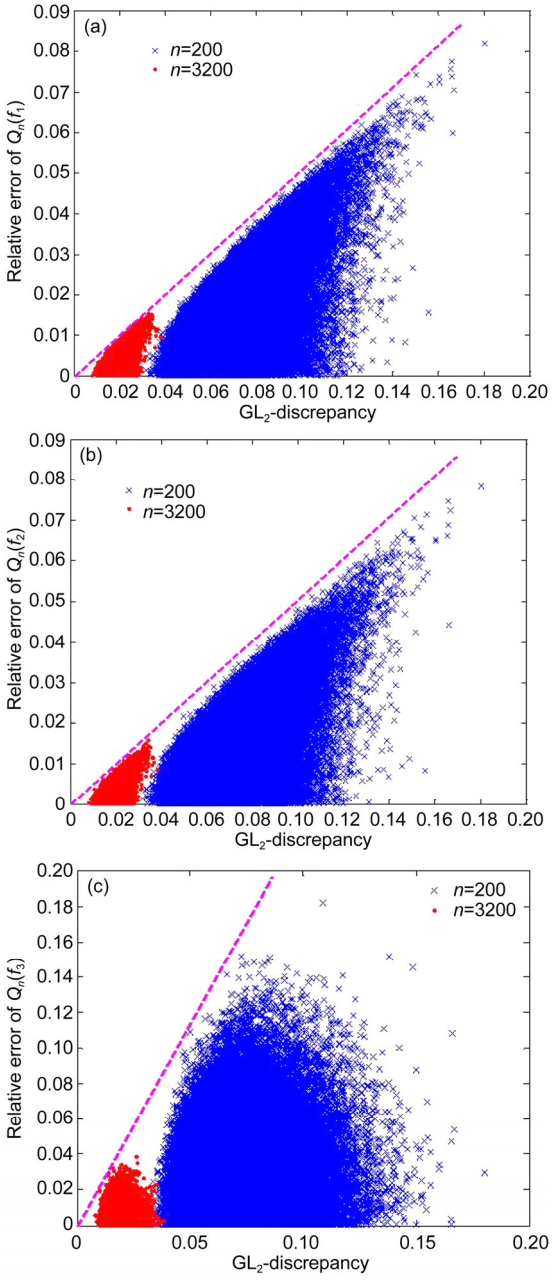


**Figure 2** (Color online) Relative error of cubature v.s. $\mathrm{GL}_2$-discrepanc. (a) Relative error of $Q_n(f_1)$ v.s. $\mathrm{GL}_2$-discrepancy; (b) relative error of $Q_n(f_2)$ v.s. $\mathrm{GL}_2$-discrepancy; (c) relative error of $Q_n(f_3)$ v.s. $\mathrm{GL}_2$-discrepancy.

inequality $e(f, M_n) \leqslant \alpha L_2^{\mathrm{uw}}(M_n)$ holds for each figure. It is seen that in different figures the coefficient $\alpha$ is different, implying that it is dependent on the integrand. This is nothing but a numerical embodiment of the extended Koksma-Hlawka inequality in Theorem 1. Another remarkable property of the figures is the scale similarity. It is seen from the figures that the areas scattered by the data pairs with different cardinal numbers for the same function resemble in shape but are different in size. This property is in a degree the manifestation that the change tendency of the accuracy and that of $GL_2$-discrepancy against the cardinal numbers almost coincide, which will also be discussed soon later. But the shapes of the scattered areas of the data pairs for different integrand functions are different: those for $f_1$ and $f_2$ (see Figure 2(a) and (b)) are more acute at the left-low corner but those for $f_3$ are blunter (see Figure 2(c)). It will be seen later that this just implies that the accuracy of cubature for $f_1$ and $f_2$ is higher than that for $f_3$ when the same representative point set is adopted, which is due to the effect of 2-norm of the integrands as shown in Theorem 1, which characterizes the degree of irregularity of the integrand in a sense.

Shown in Figure 3 are the relative errors and $GL_2$-discrepancies against the cardinal numbers. For comparison the curves of $y = n^{-1/2}$ and $y = n^{-1}(\log n)^s$ (for $s$ = 3) are also plotted. It is observed that the mean of the relative errors of the cubature for different integrands against cardinal number is in the order of $\mathcal{O}(n^{-1/2})$ (with almost the same slope in the logarithmic coordinates). The mean of $GL_2$-discrepancies for different cardinal numbers also changes in the same tendency, and happens to coincide almost exactly with the curve $y = n^{-1/2}$. But from the figure it is also seen that there is a large gap between the maximum and the minimum of $GL_2$-discrepancies for the same cardinal numbers. Note that as pointed out in the preceding section, what is really of interest is the minimal $GL_2$-discrepancies, which is obviously smaller than the mean by several times as observed in Figure 3. Besides, an almost extremely linear relationship could be observed in the mean relative errors versus mean $GL_2$-discrepancy (see Figure 4). Combining Figures 3 and 4 the scaling property for different cardinal numbers shown in Figure 2 could be interpreted in the sense of average. Of course, the description and interpretation of the scaling property in a more rigorous sense may be given by an elaborated theoretical analysis but is still left to be done.

From the above figures the tendency of the error against the cardinal numbers and the error versus the $GL_2$-discrepancy could be observed. But as pointed out in the preceding section, what is done for a practical application is to first determine a point set with the prescribed cardinal number by minimizing the $GL_2$-discrepancy, thus the error corresponding to the minimal $GL_2$-discrepancy is of real concern. First, the smallest 100 $GL_2$-discrepancies are specified and the means of these 100 values are denoted as 100-min mean $GL_2$-discrepancy for a prescribed cardinal number. Accordingly 100 data pairs could be singled out from Figure 2, and the mean of the 100 corresponding errors is labeled as "100-min mean error". By doing so, Figure 5 is plotted. It is seen that the 100-min mean error is much smaller than the mean error by nearly one order of magnitude. In Figure 6 shown are the relative errors corresponding to the point sets with the minimal (of course only nominal minimal) $GL_2$-discrepancy for the prescribed cardinal numbers. Although not a rigorous straight line, the curves in Figure 6(a) and (b) show a clear tendency of decreasing of the relative errors against decreasing of the minimal $GL_2$-discrepancies. Again from the figures, it is observed that the relative errors for $f_3$ are relatively large, as also pointed out in the preceding paragraph and in ref. [29]. The relative errors shown in Figure 6 are also plotted in Figure 7 by showing its change against the cardinal number. For comparison, the curves of $y = n^{-1/2}$ and $y = n^{-1}(\log n)^s$ are also plotted. Again, not rigorously but a tendency of decreasing of the

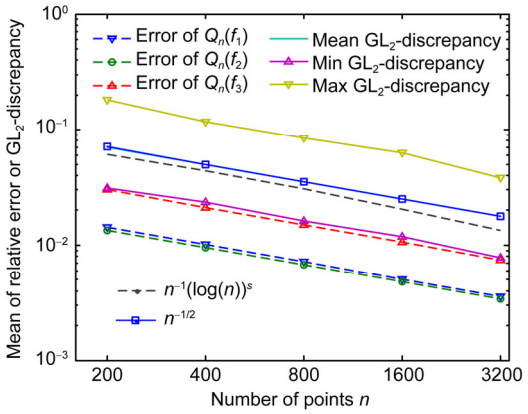


**Figure 3** (Color online) Relative error or $GL_2$-discrepancy against the cardinal numbers.

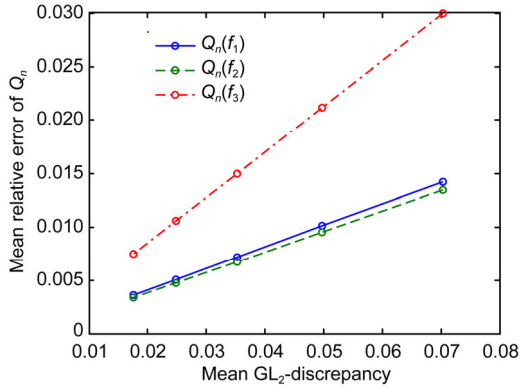


**Figure 4** (Color online) The mean relative error v.s. the mean $GL_2$-discrepancy.

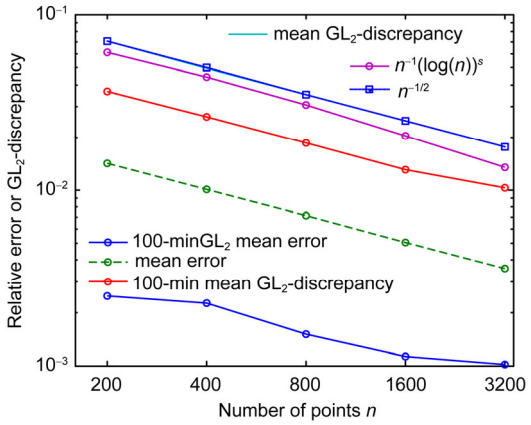


**Figure 5** (Color online) 100-min $GL_2$-discrepancy and the corresponding mean error.

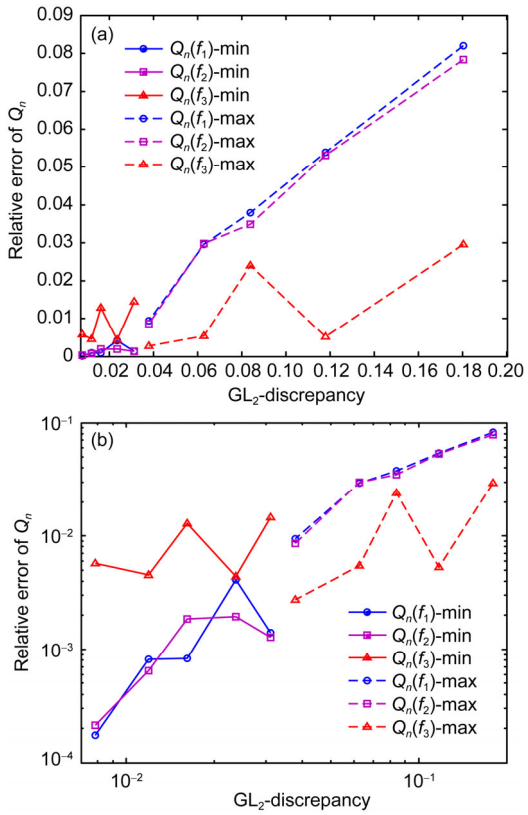


**Figure 6** (Color online) Minimal $GL_2$-discrepancy and the corresponding relative error. (a) In an ordinary coordinate system; (b) in a logrithmic coordinate system.

errors against the cardinal numbers is observed. To compare with the Monte Carlo simulation, the errors shown in Figure 8 are plotted together with 10 rounds of Monte Carlo simulation. Clearly, it is seen that the error by the proposed approach is smaller than most of the errors by Monte Carlo simulation. It is noted that the effect of the proposed approach for $f_3$ (see Figure 8(c)) is a little bit worse, which is due to the property of $f_3$ as discussed in ref. [29].

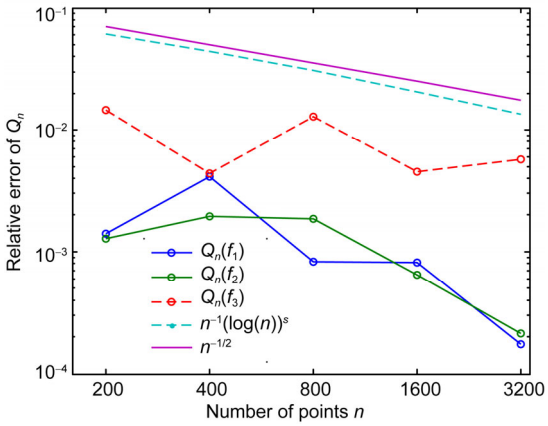


**Figure 7** (Color online) The relative errors against cardinal numbers.

It is also noted from Figures 5 through 8 that the effect of the proposed approach for small cardinal numbers (say, $n$ = 200) is even more satisfactory than the greater cardinal numbers. This is of great interest because, as mentioned previously, in many engineering practice it is required that the number of the deterministic function evaluation is at most in the order of the magnitude of 200 through 300.

### 5.2 Stochastic dynamics of nonlinear structures

For illustration, the proposed approach is now applied to the stochastic dynamic response analysis of a 10-DOF nonlinear structure subjected to seismic excitations. Some parameters of the structure are random variables. The mean values of the 10 lumped masses $m_1, m_2, \cdots, m_{10}$ and the 10 initial inter-story stiffness values $K_1, K_2, \cdots, K_{10}$ are listed in Table 1. Two uniformly distributed independent random variables $\Gamma_1$ and $\Gamma_2$ are adopted to characterize the randomness in the lumped masses, i.e., $m_i = \mu_{m_i}[1+2\sqrt{3}\delta_m(\Gamma_1 - 0.5)]$ for $1 \leqslant i \leqslant 6$ and $m_i = \mu_{m_i}[1+ 2\sqrt{3}\delta_m(\Gamma_2 - 0.5)]$ for $7 \leqslant i \leqslant 10$. Likewise, for the inter-story stiffness, another two uniformly distributed independent random variables $\Gamma_3$ and $\Gamma_4$ are involved such that $K_i = \mu_{K_i}[1 + 2\sqrt{3}\delta_K(\Gamma_3 - 0.5)]$ for $1 \leqslant i \leqslant 6$ and $K_i = \mu_{K_i}[1+2\sqrt{3}\delta_K(\Gamma_4 - 0.5)]$ for $7 \leqslant i \leqslant 10$. Here $\mu_{m_i}$ and $\mu_{K_i}$ are the mean values of the lumped masses and inter-story stiffness listed in Table 1, $\delta_m$ and $\delta_K$ are the coefficients of variation of mass and stiffness, respectively, $\Gamma_1, \Gamma_2, \Gamma_3$, and $\Gamma_4$ are four independent random variables uniformly distributed over $[0,1]$. The Bouc-Wen model [30,31] is adopted to model the hysteretic restoring force where 13 parameters, denoted by $\alpha, A, n, \beta, \gamma, d_v, d_\eta$, $\phi, q, p, d_\phi, \lambda$, and $\zeta$ (the meanings of the parameters could be found in ref. [20]),

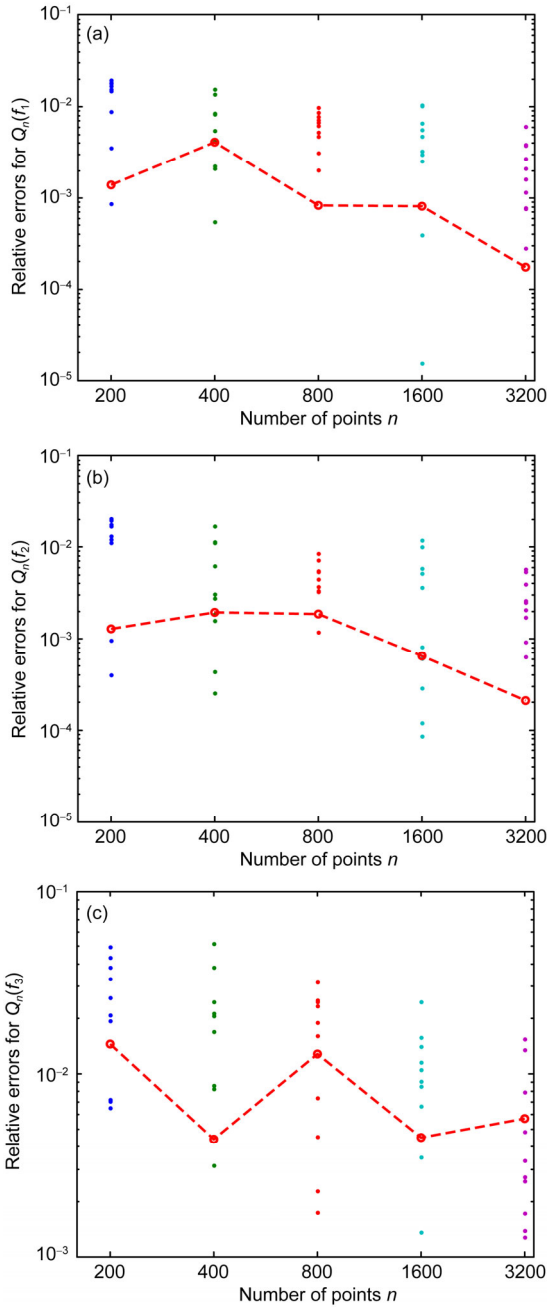


**Figure 8** (Color online) Errors of 10 MCS and the error by the proposed approach. (a) Error for $Q_n(f_1)$; (b) error for $Q_n(f_2)$; (c) error for $Q_n(f_3)$.

are involved. In the present paper, the following parameters take deterministic values: $\alpha = 0.01$, $A = 1$, $n = 1$, $q = 0$, $p = 600$, $\phi = 0.2$, $d_\phi = 0$, $\lambda = 0.5$ and $\zeta = 0.95$. The rest 4 parameters are regarded as uniformly distributed independent random variables with the mean values $E[\beta, \gamma, d_v, d_\eta] = [60, 10, 200, 200]$. The ground acceleration input is taken as $\ddot{X}_g(t) = \chi_1 a_1(t) + \chi_2 a_2(t)$, where $a_1(t)$ and $a_2(t)$ are two deterministic time histories taking the El Centro accelerograms in the North-South and East-West directions, rescaled with the peak being 3.5 m/s$^2$, respectively, and $\chi_1$ and $\chi_2$ are two uniformly distributed independent random variables with the mean values of 1. Totally ten random variables are involved. The coefficients of variation of all the random variables are set to be 0.3. This means a large variation in the parameters. It is well known that stochastic dynamics of such MDOF nonlinear systems with a large degree of variation in the parameters is still a great challenge [32,20]. In the past decade, a family of probability density evolution method (PDEM) was developed and by the point evolution scheme a representative point set with the assigned probabilities is in need [33]. Therefore, the proposed approach could be incorporated into the PDEM. The PDEM will not be elaborated here due to the length and topic of the present paper. For details, refer to [20,33].

A typical curve of the restoring force v.s. inter-story drift is shown in Figure 9, which implies that the strong nonlinearity is involved in the mechanical behavior of the structure. The time histories of the mean and standard deviation of the top displacement by the proposed method (legend "PDEM") and the Monte Carlo simulation ("MCS") are pictured in Figure 10. 300 representative points are generated by the proposed approach in the preceding section and $10^4$ times of Monte Carlo simulations are performed for comparison. Good agreement is observed, but the proposed method is more efficient by tens of times than the MCS. Actually the relative errors of the 2-norm of the mean and standard deviation process are 0.029 and 0.027, respectively. Shown in Figure 11 are the PDFs at three typical instants of time, the PDF evolution surface at a certain time interval and the corresponding contours. It is seen clearly that due to the

**Table 1** Mean of the lumped mass and stiffness

| Story No. | 1 | 2 | 3 | 4 | 5 | 6 | 7 | 8 | 9 | 10 |
|---|---|---|---|---|---|---|---|---|---|---|
| Mass ($10^5$ kg) | 1.4 | 1.4 | 1.4 | 1.3 | 1.2 | 1.2 | 1.1 | 1.0 | 1.0 | 0.7 |
| Stiffness (N/m) | 3.35 | 3.35 | 3.35 | 3.35 | 3.35 | 3.2 | 3.2 | 3.2 | 3.0 | 3.3 |

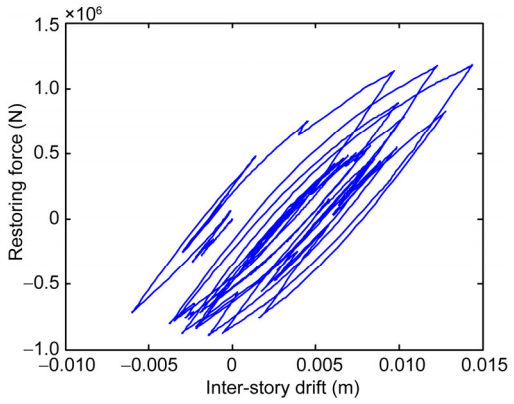


**Figure 9** (Color online) A typical curve of restoring force v.s. inter-story drift.

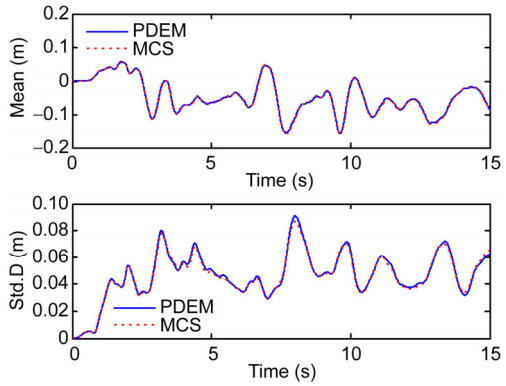


**Figure 10** (Color online) The mean and standard deviation of top displacement.

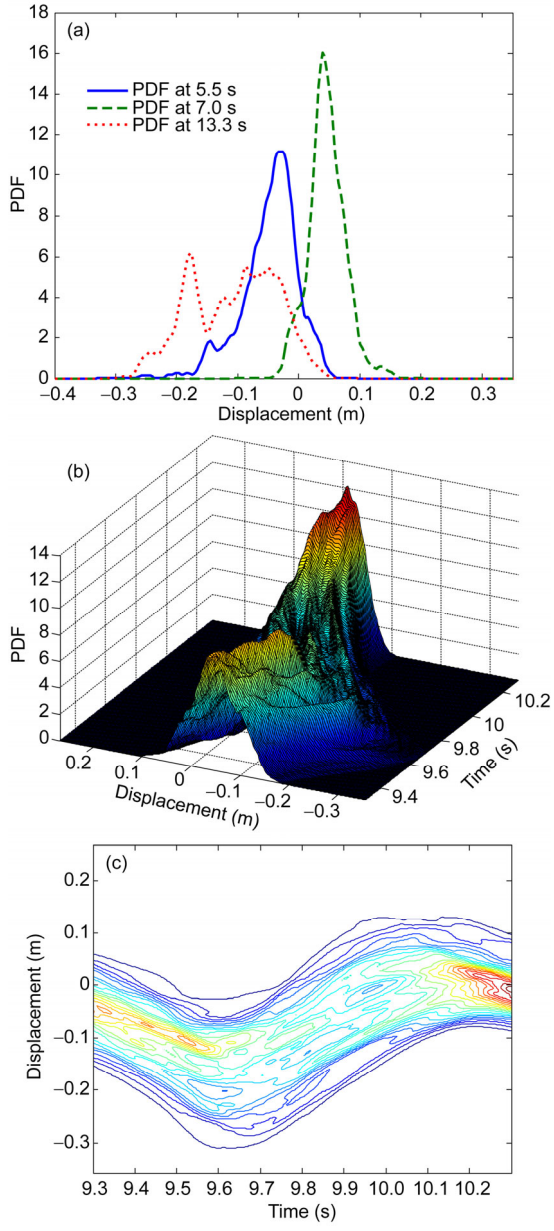


**Figure 11** (Color online) PDF surface and the contour in a specified interval. (a) PDF at three typical instants of time; (b) PDF surface; (c) contour.

nonlinearity between the response and the random variables, even the random variables follow uniform distributions, the PDF of the response is in no sense close to uniform distribution, neither close to normal distribution. These results show that the proposed approach could be applied successfully in stochastic dynamics of large MDOF nonlinear structures.

It is noted that in engineering practice, the constitutive laws of materials, such as the damage constitutive law of concrete [5] and the plastic constitutive law of rockfill materials involving the effects of density and pressure [6,7], are usually quite complex. Thereby the advanced modern nonlinear finite element method or other discretization approaches should be incorporated. Fortunately, because the embedded physical/mechanical mechanism of the system is explicitly involved in the probability density evolution method by embedding deterministic analyses, as was also pointed out in ref. [32], the extension from the present example to such practical applications is feasible. A most recent example of extension to concrete structures with the damage constitutive law could be found in ref. [34].

## 6 Concluding remarks

A generalized $L_2$-discrepancy for the point sets involving unequal weights is introduced. The extended Koksma-Hlawka inequality is proved and the closed-form expressions of the generalized $L_2$-discrepancy are given. An algorithm for the optimal point selection by minimizing the generalized $L_2$-discrepancy is proposed. Numerical examples are studied to expose the property of the point sets and the error estimate of the cubature formulas. The proposed method is incorporated into the probability density evolution method to implement the stochastic dynamic response analysis of an MDOF nonlinear structure. It is also noted that once the point sets are generated, they could be stored or tabulated and then be applied to other problems because of their non-problem-specific property.

Problems to be further studied include: (1) Applications of the advanced optimization methods for search of the optimal values of coordinates and unequal weights; (2) the extension of the proposed idea to scenario involving multiple non-uniform distributed random variables; and (3) the extension of the proposed idea to the practical applications involving such materials as concrete or rockfill materials with complex constitutive laws.

*This work was supported by the National Natural Science Foundation of China (Grant Nos. 51538010 & 51261120374), the State Key Laboratory of Disaster Reduction in Civil Engineering (Grant No. SLDRCE14-B-17), and the Fundamental Funding for Central Universities.*

1 Brandolini L, Colzani L, Gigante G, et al. On the Koksma–Hlawka

inequality. J Complexity, 2013, 29: 158–172
2 Bungartz H J, Griebel M. Sparse grids. Acta Numer, 2004, 13: 1–123
3 Chen J B, Li J. Strategy for selecting representative points via tangent spheres in the probability density evolution method. Int J Numer Meth Eng, 2008, 74: 1988–2014
4 Wriggers P. Nonlinear Finite Element Methods. Berlin Heidelberg: Springer-Verlag, 2008
5 Li J, Wu J Y, Chen J B. Stochastic Damage Mechanics of Concrete Structures (in Chinese). Beijing: Science Press, 2014
6 Xiao Y, Liu H L, Chen Y M, et al. Bounding surface model for rockfill materials dependent on density and pressure under triaxial stress conditions. J Eng Mech, 2014, 140: 04014002
7 Xiao Y, Liu H L, Chen Y M, et al. Bounding surface plasticity model incorporating the state pressure index for rockfill materials. J Eng Mech, 2014, 140: 04014087
8 Xiu D B. Fast numerical methods for stochastic computations: A review. Commun Comput Phys, 2009, 5: 242–272
9 Tang T, Zhou T. Recent developments in high order numerical methods for uncertainty quantification (in Chinese). Sci China Math, 2015, 45: 891–928
10 Smolyak S. Quadrature and interpolation formulas for tensor products of certain classes of functions. Soviet Math Dokl, 1963, 4: 240–243
11 Genz A. Fully symmetric interpolatory rules for multiple integrals. SIAM J Numer Anal, 1986, 23: 1273–1283
12 Xu J, Chen J, Li J. Probability density evolution analysis of engineering structures via cubature points. Comput Mech, 2012, 50: 135–156
13 Victoir V. Asymmetric cubature formulae with few points in high dimension for symmetric measures, SIAM J Numer, 2004, 42: 209–227
14 Chen J B, Zhang S H. Improving point selection in cubature by a new discrepancy. SIAM J Sci Comput, 2013, 35: A2121–A2149
15 Hua L K, Wang Y. Applications of Number Theory to Numerical Analysis. Berlin Heidelberg: Springer-Verlag, 1981
16 Fang K T, Wang Y. Number-theoretic Methods in Statistics. London: Chapman & Hall, 1994
17 Niederreiter H. Random Number Generation and Quasi-Monte Carlo methods. Philadelphia, Pennsylvania: SIAM, 1992
18 Dick J, Kuo F Y, Sloan I H. High-dimensional integration: the quasi-Monte Carlo way. Acta Numerica, 2013, 133–288
19 Dick J, Pillichshammer F. Digital Nets and Sequences. Cambridge: Cambridge University Press, 2010
20 Li J, Chen J B. Stochastic Dynamics of Structures. Chichester: John Wiley & Sons Ltd., 2009
21 Proinov P D. Generalization of two results of the theory of uniform distribution. P Am Math Soc, 1985, 95: 527–534
22 Hickernell F J, Wozniakowski H. Integration and approximation in arbitrary dimensions. Adv Comput Math, 2000, 12: 25–58
23 Novak R, Wozniakowski H. $L_2$ discrepancy and multivariate integration. Analytical Number Theory: Essays in Honor of Klaus Roth. Chen W W L, Gowers W T, Halberstam H, et al., eds, Cambridge: Cambridge University Press, 2009. 359–388
24 Chen J B, Ghanem R, Li J. Partition of the probability-assigned space in probability density evolution analysis of nonlinear stochastic structures. Probabilist Eng Mech, 2009, 24: 27–42
25 Chen J B, Yang J Y, Li J. A GF-discrepancy for point selection in stochastic seismic response analysis of structures with uncertain parameters. Struct Saf, 2016, 59: 20–31
26 Nocedal J, Wright S J. Numerical Optimization. New York: Springer, 1999
27 Roberts J B, Spanos P D. Random Vibration and Statistical Linearization. Chichester: John Wiley & Sons Ltd., 1990
28 Song P Y, Chen J B. Point selection strategy based on minimizing $GL_2$-discrepancy and its application to multi-dimensional numerical integration (in Chinese). Sci Sin Tech, 2015, 45: 547–558
29 Wang X, Hickernell F J. Randomized Halton sequences. Math Comput Model, 2000, 32: 887–899
30 Wen Y K. Method for random vibration of hysteretic systems. J Eng Mech, 1976, 102: 249–263
31 Ma F, Zhang H, Bockstedte A, et al. Parameter analysis of the differential model of hysteresis. J Appl Mech, 2004, 71: 342–349
32 Goller B, Pradlwarter H J, Schueller G I. Reliability assessment in structural dynamics. J Sound Vib, 2013, 332: 2488–2499
33 Li J, Chen J, Sun W, et al. Advances of probability density evolution method for nonlinear stochastic systems. Probabilist Eng Mech, 2012, 28: 132–142
34 Song P Y, Chen J B, Wan Z Y, et al. Probability density evolution analysis of stochastic seismic response of concrete frame structures (in Chinese). J Building Struct, 2015, 36: 117–123